A NEW APPROACH TO WINDING DISPLACEMENT DETECTION OF POWER TRANSFORMER USING FRA METHOD AND ELECTRICAL FORCES DISTRIBUTION

Ali Shirvani Boroujeni Gevorg B. Gharehpetian Mohammad Nazari
e-mail:alishirvani@aut.ac.ir grptian@aut.ac.ir mohammadnazari@dena.aut.ac.ir
Amirkabir University of Technology, Department of Electrical & Electronics Engineering, 424 Hafez Ave, 15914 Tehran, Iran

Key word: power transformer, winding deformation, diagnosis, FRA, electrical forces

ABSTRACT

Electrical forces during Short circuit or impulse lighting can cause mechanical displacements of transformer windings. The electrical forces distribution on transformer winding is used as a helpful tool for FRA method to a better and faster detection of exact location of winding displacement. In order to be able to evaluate the measurements, the correlation between the characteristics of transfer functions and possible damages must be known. The detailed mathematical models were developed for the test objects and a comparison was carried out between different results. It is shown that this method can detect the exact location of deformation in transformer windings.

I. INTRODUCTION

High voltage transformer is one of the most essential and important element of electric power systems. Their breakdown may lead to an abrupt breakdown of overall system and thus, in proportion of their importance, their protections are essential.

It is desirable to detect potential failure as early as possible. The main aims are, on one hand, to check the actual health state of a particular transformer in order to predict the breakdown before it occurs, and on the other hand, to decide whether to repair a transformer or not (for instant just after lighting). In this regard, several procedures such as thermal monitoring, oil analyzes, partial discharge measurements, transfer function, relaxation current, recovery voltage measurement and etc., are investigated and applied. It is also clear that each method can be applied for a specific type of problems and has its own merits.

The frequency response analysis test (FRA) is increasingly being used to detect winding movement and distortion [1]-[9]. Since the electrical changes corresponding to mechanical deformations are notably observed in those frequency responses, much research has been carried out, on FRA [4], [5] or the transfer function method (TFM) [6], [7]. In the FRA test the transformer is isolated from the system and a wide bandwidth signal is applied to one winding terminal and the response is measured at another terminal. The magnitude of the neutral current of the transformer is calculated as a function of frequency. This gives a “fingerprint” of the transformer. The tests are repeated over time and the fingerprints are compared. Transfer function variations are used as a tool to recognize mechanical displacements and deformation of windings [1], but determining the exact location and the extent of these faults is the subject to active research. The suitability of this method was confirmed in several experiments on power transformers in service [8], [9]. All the existing FRA methods have utilized the frequency range of a few tens of kHz to about 1 MHz.

It is known that mechanical deformations arise mainly due to short-circuit and impulse forces, unskilled handling, and rough transportation. But in this research, only the deformations that lead from electrical forces are investigated. In this manner, the electrical force distribution on the winding are calculated and based on the maximum force, the points with high probability of deformation are identified. After the identification of candidate points in the HV windings, in the next step with FRA method, the exact location among the candidate points and the extent of faults are declared.

Although the information related to winding deformation is embedded in the TF, using electrical force distribution, as an additional method, brings out two main benefits. Firstly, it is possible that two distinct deformations lead same change in TF from and therefore, this problem can leads to incorrect detection. Secondly, instead of analyzing all of the possible case of deformation, identification of probable locations of deformation decreases the search domain.

Hence, to ensure accurate diagnosis and to save the time, the presented procedure uses electrical forces for exact

diagnosis. For the firs step, correct interpretation of TF and electrical forces should be prepared. Then, regards to the accident (short circuited, lighting impulse or etc.) that is happened for the transformer, distribution of electrical force on the HV winding are calculated and locations with high probability of displacement are identified. Finally with the aid of FRA method and regarded to the candidate locations, the exact location of deformation are declared.

This paper is organized as follows: after this introduction, in the next section, a detailed model for the transformer is proposed and the relations among the model parameters and the different internal parts of the transformer are presented. In section III, All factors and/or interactions that affect short-circuit forces are taken into account and to achieve systematic diagnostic procedure, an appropriate method for calculating forces is presented. Section IV explains diagnostic procedure and detailed test setup and experiments. The diagnostic results on simulated faults using all discrimination criteria are presented in section V. Finally, Section VI concludes our work and discusses future work.

II. TRANSFORMER DETAILED MODEL

There has been a great deal of research on transformer modeling using a variety of models [10]–[14]. Principally, there are three main categories of models: I) terminal or black box model, II) Physical models and III) Combination of Black-Box and physical model [10].

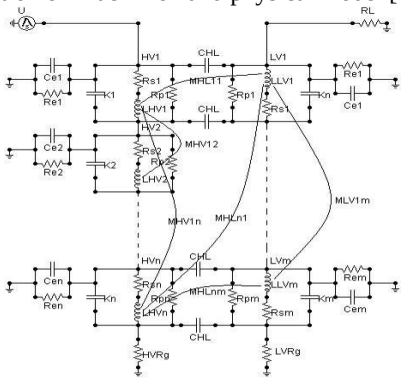

Figure 1- Detailed model of transformer

The Black-Box models such as Modal analyze [11] and Description by pole and zeros method [12] provides the terminal characteristics of a transformer that is not necessarily related to a transformer internal condition and physical configuration. These models are used when the transformer consider as one part of the bigger network. In such conditions the main focus is not on the transformer. In the other word, black box model is mainly used for system performance studies rather than transformer internal changes. Therefore, these models are not suitable for the modeling of winding displacements. In the other hand, the physical model like phase transmission line model [13] or detailed model[14], are based on the geometry of the winding and its lumped equivalent circuit. They can either model all parts of the transformer in great detail or can be constructed according to gross physical components such as the winding layers. These types of models use network equivalent parameters (RLC) and focus on the frequency range of interest.

As the goal of the present investigation involved the study of TF, the detailed model based on a completely coupled ladder network circuit model is preferred. It has widely been used in the past and also is known to accurately model all aspects of the neutral current response due to lightning impulses. In addition, this representation readily permits computation of time-domain responses using circuit simulation software (PSPICE or EMTP), and also construction of a winding model for experimental verification. This model is also valid for higher frequencies.

The equivalent circuit diagram of the test objects beyond 10 kHz is shown in Fig. 1. A winding unit can contain one disk, two disks or several numbers of turns. The number of units is a modeling parameter and the chosen value is a compromise between the accuracy and the complexity.

As a test object for the study of axial displacement, a high voltage winding with 28 double disks, 18 turns in each disk, and a four layer concentric low voltage winding, 90 turns in each layer, were used. These particular windings have the construction of transformer windings with a rated voltage of 230/63 kV and 160KVA. The test object has 150 cm height and 90 cm diameter.

Each winding was represented by a coupled ladder network circuit comprising of series capacitance (K_1, K_2, K_n, K_m), series inductance ($L_{HV1}, L_{HVn}, L_{LV1}, L_{LVm}$), shunt capacitances ($C_{e1}, C_{en}, C_{em}$), inter-winding capacitance (C_{HL}), all mutual inductances between each section of a winding (M_{HV12}, M_{LV1m}), and all mutual inductances between the two windings M_{HLnm}. Loss in the winding and insulation losses was modeled by lumped resistances (R_{sn}, R_{sm}) in series with series inductance and lumped resistances ($R_{pn}, R_{pm}, R_{en}, R_{em}$) in parallel with series and shunt capacitances in both windings.

The elements of the circuit diagram are defined in [15]. Model parameters are calculated analytically after some simplifications of the geometrical structure of the winding.

A. Self and Mutual Inductance

The self and mutual inductance can be calculated by the solution of vector potential method. The calculation of the mutual inductance of the arrangement as sketched in Fig. 2 is explained in [3]:

$$M_{12} = \frac{2\mu_0\sqrt{r_1 r_2}}{\sqrt{k'}}.[K(k') - E(k')] \qquad (1)$$

Where:

$$k' = \frac{1-\sqrt{1-k^2}}{1+\sqrt{1-k^2}} \quad , \quad k = \sqrt{\frac{4r_1 r_2}{(r_1+r_2)^2 + d^2}}$$

$E(k')$ and $K(k')$ are the first and second kind of the complete elliptical integrals. r_1 and r_2 are the radii of the interesting turns.

For calculating the mutual inductance between two windings with n and m turn in each winding, the mutual

inductance between every two turn must be added as follows:

$$M_{12} = \sum_{i=1}^{n} \sum_{j=1}^{m} M_{12}(i, j) \qquad (2)$$

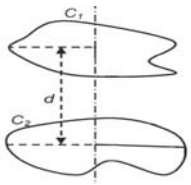

Figure 2- Two parallel conducting loops

Where $M_{12}(i, j)$ is the mutual inductance of the i[th] turn of the winding 1 and j[th] turn of the winding 2 and calculate from (3).

For example, if a 5 cm axial displacement occurs from 8[th] Unit, mutual inductance of sections will be changed. The calculated inductance of some double discs and LV winding, are given in table I. Self inductances are not changed because such displacements do not affect on the arrangement of sections. But some mutual inductances are decreased as a result of increasing the relative axial distance of different sections.

Table I.
SOME TYPICAL ELEMENTS OF INDUCTANCE MATRIX OF THE TEST TRANSFORMER BEFORE AND AFTER WINDING DISPLACMENT

Self and mutual inductance(μH)	4[th] HV D-Disc		1[st] LV layer	
	Before Displacement	After Displacement	Before Displacement	After Displacement
4[th] HV D-Disc	4.2115	2.8185	2.6093	
24[th] HV D-Disc	0.83701	0.77723	2.904	2.7206
1[st] LV layer	2.8185	2.6093	8.8768	

B. Capacitance

The longitudinal capacitances which present electrostatically stored energy between the turns of a winding unit, are difficult to be calculated analytically. The principle of capacitance calculation will be demonstrated on ordinary disc-type windings. In Fig. 3, the schematic drawing of a double-disc coil consisting of two sections and its capacitance network is shown. The series capacitance of this disc coil is composed of two parts, being the resultant of inter-turn capacitances C_t and the inter-section capacitances C_d. The calculation of the resultant capacitance of the disc coil is based on the principle that the sum of energies accumulated in the part capacitances within the section is equal to the entire energy of the disc coil.

If the mean winding diameter is D, the size of copper conductor used for calculating the turn-capacitance is h, the thickness of inter-turn insulation is δ_t and its permittivity is ε_t, the radial size of winding is r, the thickness of spacers between discs is δ_d and the resultant permittivity of (oil + solid) insulation of thickness δ_d is ε_d (notations shown in Fig. 3), then the inter-turn capacitance C_t and the inter-disc capacitance C_d can be calculated from the known formula for plane condensers as follows:

$$C_{dr} = \frac{1}{3}\varepsilon_0 D\pi \frac{r+\delta_d}{\left(\frac{2\delta_t}{\varepsilon_t} + \frac{\delta_d}{\varepsilon_d}\right)}, C_t = \varepsilon_t \varepsilon_0 \frac{D\pi(h+2\delta_t)}{2\delta_t} \qquad (3)$$

On the basis of relation (3), after some mathematical manipulations, the series capacitance of normal disc windings can be calculated from the equation:

$$K = \frac{27.8D}{N}\left(\frac{\varepsilon_t(h+2\delta_t)}{2n\delta_t} + \frac{4}{3}\frac{r+\delta_d}{\frac{2\delta_t}{\varepsilon_t} + \frac{\delta_d}{\varepsilon_d}}\right) 10^{-12}\, F \qquad (4)$$

Where n is the number of turns per disc, and N is the number of discs in winding.

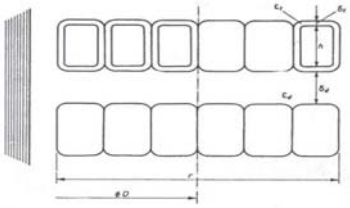

Figure 3- letter symbols used in the calculation of series capacitance of disc coils

Parallel capacitance C_{ei} presents the electrical field between individual disk units and earth (tank or core) as well as the electrical field between different windings C_{HL}. Considering the dimension of the windings, the calculation of these capacitances can be done based on a cylindrical or a homogeneous distribution of the electrical field. However, an appropriate correction factor is necessary for the edge effects.

The calculated series and shunt capacitances, before and after a 5 cm axial displacement in 8[th] Unit of HV winding, are given in table II.

Table II.
THE CALCULATED CAPACITANCE BETWEEN TWO WINDINGS OF THE TRANSFORMER BEFORE AND AFTER WINDING DISPLACMENT

CAPACITANCE(nF)	Before displacement	After displacement
K_{HV8}	0.95504	0.74172
K_{LV}	0.383	
C_{HL}	3.3689	3.4008
C_{eHV}	1.0341	1.1037
C_{eLV}	6.2957	

C_{eLV} and K_{LV} are not changed because such displacements do not affect on the arrangement of LV layer. But as a result of the axial distance rising of 8[th] Unit from other sections, K_{HV8} are decreased. Also because of increasing the overall height of HV winding, C_{HL} and C_{eHV} are increased.

C. Resistances

Electric and magnetic behavior of transformer windings is the subject to the damping mechanisms due to core losses and losses in windings and insulations. At higher frequencies (>10 kHz for power transformers) the magnetic penetration depth is so low that the core losses can be neglected. Rs_i represents the conductor resistance

with skin and proximity effects. Rp_i and Re_i represent the dielectric losses between winding turns and between winding and tank (or other windings or core) respectively, and both of them are frequency dependent. The calculation of these resistances is explained thoroughly in [3].

III. SHORT-CIRCUIT FORCES CALCULATION

The force between these coils can be calculated with different methods. Some of them use mutual inductance between coils and its derivative [16]. This paper deals with another method in which the results are expressed over the complete elliptical of the first and second. In order to apply detailed model of transformer and for being in harmony with calculation of inductances, this method has been chosen. Therefore the transformer winding is divided into circular coils and loops and the force between the coils has been calculated using Magnetic analysis. Therefore only the number of turns and dimension of windings will be considered. The calculation of the electrical forces of the arrangement as sketched in Fig. 2 is explained in [16]-[18]:

$$F_{12} = -a_z \frac{\mu_0 r_1 r_2 I_1 I_2 dk}{2\sqrt{r_1 r_2}(1-k^2)} \cdot \left((1-k^2)K(k) - (1-\frac{1}{2}k)E(k) \right) \quad (5)$$

Finally, the total axial force of a unit with n turn can be calculated as follow:

$$F_i = \sum^{i} \sum^{j} F(i,j) \quad (6)$$

Where $F(i,j)$ is the axial force between ith turn of selected section and jth turn of other winding turns and can be calculated from (5).

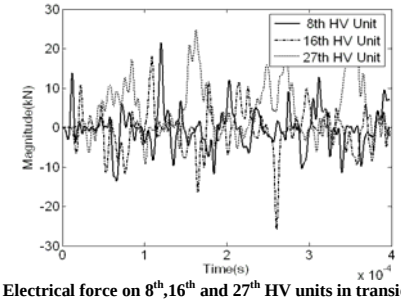

Figure 4- Electrical force on 8th,16th and 27th HV units in transient mode

In normal conditions, axial forces increased when move from centre of transformer to its edges. But in transient modes, because of disturbance in currents, axial forces are more disordered. Fig. 4 shows the electrical force on 8th, 16th and 27th HV units in transient mode after lighting impulse strike.

IV. DETECTION METHOD

In the proposed method exact location of displacement is determined based on FRA and forced distribution on winding. The electrical currents of HV and LV units in circumstance of short circuit or lighting impulse are determined by simulation with EMTP and then the electrical force distribution on HV winding is extracted from (6).

At the next step, based on the force distribution, units with excessive force on them have the high probability of displacement and therefore, in this fault condition, these units will be candidate points for real displacement location. As the next step, different displacements are considered in each candidate points and related TF are obtained by simulation.

Finally, TF of faulted transformer is compared with all obtained TFs. the TF which is most similar to the reference TF is selected and related displacements recognized as real displacement.

V. SIMULATION RESULTS

For example, it is supposed that a lighting impulse is imposed to the transformer HV terminal and 16th disk (8th double disk) is displaced 5cm in axial direction. After determining model parameters, the currents must be calculated. Figure 5 shows the current of 1st, 5th, 8th and 16th HV unit.

Electrical force distribution in $t = 120,260$ and $357\mu s$ is shown Fig 6. It is clear that the maximum force is applied on 6th, 8th and 16th Units. So the candidate disks are 6th, 8th and 16th Units.

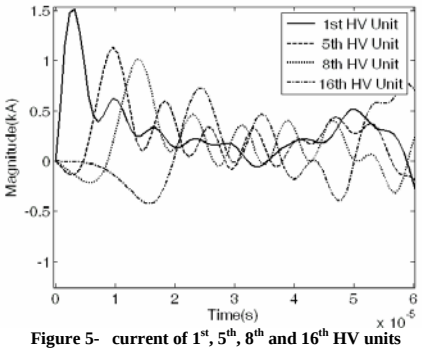

Figure 5- current of 1st, 5th, 8th and 16th HV units

In the second part of the study, the circuit in Fig. 1 was solved in EMTP using frequency domain. To simulate different location of disk displacements, simulations were repeated for different values of model parameters.

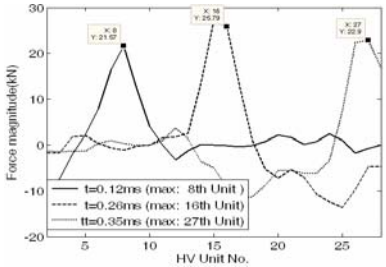

Figure 6- Force Distributin in $t = 120,260\ and\ 357\mu s$

Figure 7 shows the reference TF (a 5cm axial displacement from 16th disk) and the TFs related to a 4cm axial displacement in 8th, 16th, and 27th.

In the final step, comparison of these TFs with the reference TF can be performed in various methods such as genetic algorithm, neural network algorithm or other

classification and optimization methods. Each of these methods can be used to classify the simulated displacement regards to their TF response similarity with reference TF. In the literature of diagnosis the correlation coefficient and the standard deviation are adopted as the fingerprints of deviation between two frequency responses. The standard deviation in [19] or the root-mean-square (rms) error in [20] is computed by the following equation:

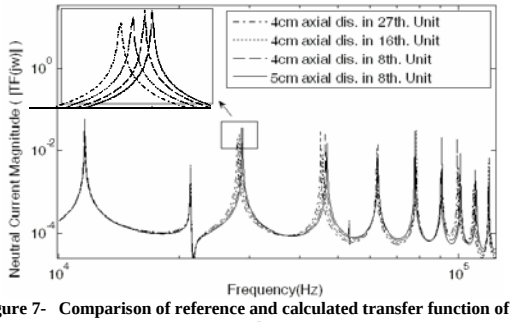

Figure 7- Comparison of reference and calculated transfer function of the earth current

$$\delta_{SSE}(x,y)=\frac{\sum_{i=1}^{N}(y_i,x_i)^2}{N} \qquad (7)$$

Where x_i and y_i are the ith elements of frequency responses to be compared, and N is the number of samples.

Based on (7), Table 4 presents the different values of δ_{SSE} for various displacements of HV winding in 8th, 16th, and 27th D-discs.

Table III.
different values of δ_{SSE} for various displacements of HV winding in 8th, 16th, and 27th D-discs

δ_{SSE}		extent			
		2cm	4cm	6cm	8cm
D-disk No.	8th	8.6214	7.1293	7.4752	8.1686
	16th	13.046	10.9138	9.0923	15.017
	27th	10.6344	9.181	11.018	10.4676

Among all of the different values of δ_{SSE}, for 4cm axial deformation, δ_{SSE8} is minimum and so expected that a 4cm axial deformation are happened in 8th D-Disk.

VI. CONCLUSION

In this paper, a novel method based Frequency Response Method and Electrical Force Distribution to detect the exact location of wining deformation and its extent has been presented. The versatility of the proposed method with reference to the number of windings, ability to represent very large number of sections and terminal conditions reported in earlier methods, was clearly illustrated.

REFERENCES

[1] T. Leibfried and K. Feser, "Monitoring of power transformers using the transfer function method," *IEEE Trans. Power Delivery*, vol. 14, no. 4, pp. 1333–1341, Oct. 1999.

[2] M. Wang, A. John Vandermaar, and K. D. Srivastava, "Improved Detection of Power Transformer Winding Movement by Extending the FRA High Frequency Range " *IEEE Trans. Power Delivery*, vol. 20, no. 3, July 2005

[3] Ebrahim Rahimpour, Jochen Christian, Kurt Feser, and Hossein Mohseni," Transfer Function Method to Diagnose Axial Displacement and Radial Deformation of Transformer Windings," *IEEE Trans. Power Delivery*, vol. 18, no. 2, pp. 493–505, April. 2003.

[4] L. Coffeen and J. Hildreth, "A new development in power transformer frequency response analysis to determine winding deformation WITHOUT the need for comparison to historical data [the objective winding asymmetry test]," in *Proc. EPRI Substation Equipment Diagnostics Conf. X*, San Antonio, TX, Feb. 2002.

[5] S. A. Ryder, "Diagnosing transformer faults using frequency response analysis," *IEEE Electr. Insul. Mag.*, vol. 19, no. 2, pp. 16–22, Mar./Apr. 2003.

[6] R. Malewski and B. Poulin, "Impulse testing of power transformers using the transfer function method," *IEEE Trans. Power Del.*, vol. 3, no. 2, pp. 476–489, Apr. 1988.

[7] S. Islam and G. Ledwich, "Locating transformer faults through sensitivity analysis of high frequency modeling using transfer function approach," in *Proc. IEEE Int. Symp. Electrical Insulation*, 1996, pp. 38–41.

[8] K. Feser, J. Christian, C. Neumann, U. Sundermann, T. Leibfried, A. Kachler, and M. Loppacher, "The transfer function method for detection of winding displacements on power transformers after transport, short circuit or 30 years of service," in CIGRE 12/33-04, 2000.

[9] J. Christian, K. Feser, U. Sundermann, and T. Leibfried, "Diagnostics of power transformers by using the transfer function method," in *Proc. 11th Int. Symp. High Voltage Eng.*, vol. 1, London, U.K., Aug. 1999, pp. 37–40.

[10] G. B. Gharehpetian, H. Mohseni, and K. Möller, "Hybrid modeling of inhomogeneous transformer windings for very fast transient overvoltage studies," *IEEE Trans. Power Delivery*, vol. 13, pp. 157–163, Jan. 1998.

[11] P. T. M. Vaessen, "Transformer model for high frequencies," *IEEE Trans. Power Delivery*, vol. 3, pp. 1761–1768, Oct. 1988.

[12] A. Morched, L. Marti, and J. Ottewangers, "A high frequency transformer model for the EMTP," *IEEE Trans. Power Delivery*, vol. 8, pp. 1615–1626, July 1993

[13] Y. Shibuya, S. Fujita, and N. Hosokawa, "Analysis of very fast transient overvoltage in transformer winding," *Proc. Inst. Elect. Eng..-Gener. Transm. Distrib.*, vol. 144, no. 5, pp. 461–468, Sept. 1997.

[14] E. Buckow, "Berechnung des Verhaltens von Leistungstransformatoren bei Resonanzanregung und Möglichkeiten des Abbaus Innerer Spannungsüberhöhungen," Ph.D., TH Darmstadt, Darmstadt, Germany, 1986.

[15] E. Rahimpour, J. Christian, K. Feser, and H. Mohseni, "Modellierung der transformatorwicklung zur Berechnung der Übertragungsfunktion für die Diagnose von Transformatoren," in *Elektrie*, Berlin, 2000, Paper no. 54/1-2, pp. 18–30.

[16] K. Fujisaki, "Magnetohydrodynamic stability in pulse electromagnetic casting", IEEE Transactions on Industry Application, Vol. 39, No. 5, Sep./Oct. 2003.

[17] T. G. Engel, D. Surls and W. C. Nunnally, "Prediction and verification of electromagnetic forces in helical coil launchers", IEEE Transactions on Magnetics, Vol. 39, No. 1, January 2003.

[18] S. Babic, C. Akyel and S. J. Salon, "New procedures for calculating the mutual inductance of the system: filamentary circular coil-massive circular solenoid", IEEE Transactions on Magnetics, Vol. 39, No. 3, May 2003.

[19] D. K. Xu, C. Z. Fu, andY. M. Li, "Application of artificial neural network to the detection of the transformer winding deformation," in *Proc. High Voltage Engineering Symp.*, 1999, pp. 5.220.P5–5.223.P5.

[20] T. McKelvey, H. Akçay, and L. Ljung, "Subspace-based multivariable system identification from frequency response data," *IEEE Trans. Autom. Control*, vol. 41, no. 7, pp. 960–979, Jul. 1996.